

J1406+0102: Dust Obscured Galaxy Hiding Super Eddington Accretion System with Bright Radio Emission

HIKARU FUKUCHI,<sup>1</sup> KOHEI ICHIKAWA,<sup>1,2</sup> MASAYUKI AKIYAMA,<sup>1</sup> SHIGEO KIMURA,<sup>1,2</sup> YOSHIKI TOBA,<sup>3,4,5</sup> KOHEI INAYOSHI,<sup>6</sup>  
AKATOKI NOBORIGUCHI,<sup>7</sup> TOSHIHIRO KAWAGUCHI,<sup>8</sup> XIAOYANG CHEN,<sup>9</sup> AND ITSNA K. FITRIANA<sup>1</sup>

<sup>1</sup>*Astronomical Institute, Tohoku University, Aramaki, Aoba-ku, Sendai, Miyagi 980-8578, Japan*

<sup>2</sup>*Frontier Research Institute for Interdisciplinary Sciences, Tohoku University, Sendai 980-8578, Japan*

<sup>3</sup>*National Astronomical Observatory of Japan, 2-21-1 Osawa, Mitaka, Tokyo 181-8588, Japan*

<sup>4</sup>*Academia Sinica Institute of Astronomy and Astrophysics, 11F of Astronomy-Mathematics Building, AS/NTU, No.1, Section 4, Roosevelt Road, Taipei 10617, Taiwan*

<sup>5</sup>*Research Center for Space and Cosmic Evolution, Ehime University, 2-5 Bunkyo-cho, Matsuyama, Ehime 790-8577, Japan*

<sup>6</sup>*Kavli Institute for Astronomy and Astrophysics, Peking University, Beijing 100871, People's Republic of China*

<sup>7</sup>*School of General Education, Shinshu University, 3-1-1 Asahi, Matsumoto, Nagano 390-8621*

<sup>8</sup>*Department of Economics, Management and Information Science, Onomichi City University, Hisayamada 1600-2, Onomichi, Hiroshima 722-8506, Japan*

<sup>9</sup>*National Astronomical Observatory of Japan, 2-21-1, Osawa, Mitaka, Tokyo 181-8588, Japan*

(Received March 13, 2023)

Submitted to ApJL

ABSTRACT

Recent high- $z$  quasar observations strongly indicate that super-Eddington accretion is a crucial phase to describe the existence of supermassive black holes (SMBHs) with  $M_{\text{BH}} \gtrsim 10^9 M_{\odot}$  at  $z \gtrsim 7$ . Motivated by the theoretical suggestion that the super-Eddington phase efficiently produces outflows and jets bright in radio bands, we search and find a super-Eddington radio-loud dust-obscured galaxy (DOG) J1406+0102 at  $z = 0.236$ , through cross-matching of the infrared-bright DOGs of Noboriguchi et al. (2019) with the VLA/FIRST 1.4 GHz radio and the SDSS optical spectral catalog. DOG J1406+0102 shows broad components in the Balmer lines. Assuming those lines are from the broad line region, it gives BH mass estimation of  $\log(M_{\text{BH}}/M_{\odot}) = 7.30 \pm 0.25$ , and AGN luminosity of  $\log(L_{\text{bol, [O III]}}/\text{erg s}^{-1}) = 45.91 \pm 0.38$  estimated from the intrinsic [O III] luminosity, resulting in super-Eddington accretion of  $\lambda_{\text{Edd}} \simeq 3$ . We show that 1) DOG J1406+0102 is operating strong AGN feedback: the [O III] outflow velocity exceeds the escape velocity of the host galaxy halo and the kinetic efficiency is obtained as  $\approx 8\%$  that can be sufficient to quench the host galaxy, 2) the expected future growth pathway of DOG J1406+0102 would join an over-massive BH trajectory and 3) radio-loud DOGs can provide a significant contribution to the high-energy ( $\gtrsim 100$  TeV) cosmic neutrino background if we assume DOG J1406+0102 as a representative of radio-loud DOGs.

*Keywords:* galaxies: SMBH growth: active — galaxies: nuclei — quasars: general

1. INTRODUCTION

Recent surveys of high- $z$  quasars have revealed that supermassive black holes (SMBHs) with mass of  $\simeq 10^9 M_{\odot}$  already exist at the redshift  $z \gtrsim 7$  (e.g., Wang et al. 2021). These sources require massive BH seeds and/or super-Eddington accretion ( $\lambda_{\text{Edd}} \equiv$

$L_{\text{AGN, bol}}/L_{\text{Edd}} \geq 1$ ) to SMBHs (e.g., Inayoshi et al. 2020), where  $L_{\text{AGN, bol}}$  is AGN bolometric luminosity and  $L_{\text{Edd}}$  is Eddington luminosity ( $L_{\text{Edd}} \simeq 1.26 \times 10^{38} (M_{\text{BH}}/M_{\odot}) \text{ erg s}^{-1}$ ). Thus, super-Eddington accreting sources are important targets for excavating the detailed BH growth, leading the intensive theoretical and observational studies (Inayoshi et al. 2020; Greene et al. 2020). However, the currently known super-Eddington sample might be only the tip of the iceberg since the super-Eddington phase is expected to last a short timescale of the order of 1-10 Myr based on ra-

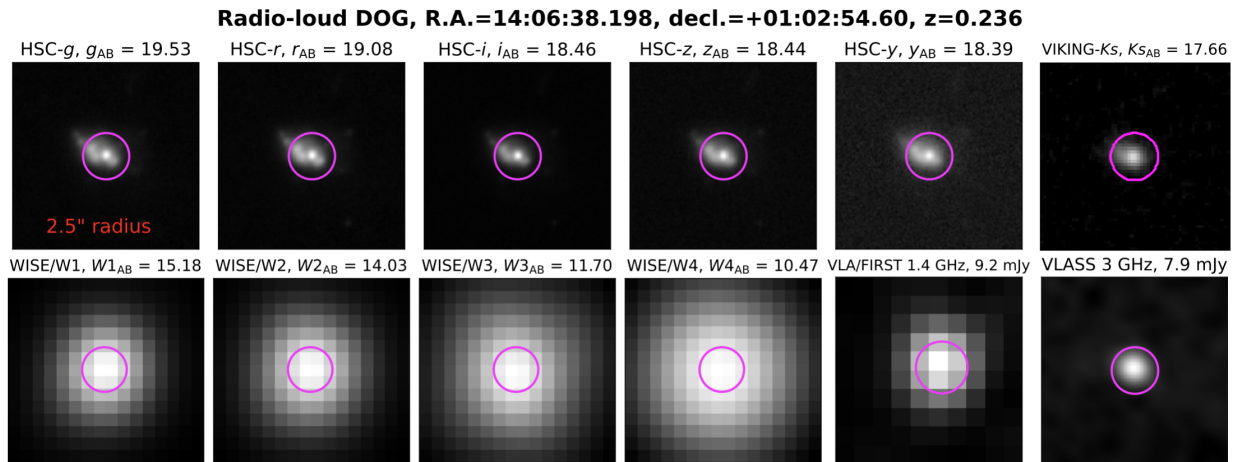


**Figure 1.** Multiwavelength cutout images for J1406. The name of each photometric band and its AB magnitude are shown above each image. The magenta circle corresponds to 2.5'' radius, which is the typical angular resolution of the VLASS survey.

diative hydrodynamic simulations (e.g., Inayoshi et al. 2022) and semi-analytic model (e.g., Shirakata et al. 2020). In addition, they are most of the time highly obscured by surrounding gas (e.g., Hopkins et al. 2008).

A major merger of two gas-rich galaxies is an efficient path to trigger rapid mass accretion onto SMBHs (e.g., Hopkins et al. 2006), although they are expected to be heavily obscured by surrounding dust, which would produce the extremely red color between the optical and infrared (IR) bands, and sometimes they are called dust-obscured galaxies (DOGs: e.g., Dey et al. 2008). Our team recently found IR-bright DOGs whose optical to IR color is extremely red with  $(i - [22]) > 7$ , where  $i$  and  $[22]$  are HSC  $i$ -band and *WISE* 22  $\mu\text{m}$  AB magnitudes (Toba et al. 2015, 2017; Noboriguchi et al. 2019) by using Subaru/Hyper Suprime-Cam (HSC: Miyazaki et al. 2018)-Subaru Strategic Program (SSP) wide-field and deep imaging data (Aihara et al. 2018) and archival IR data (ALLWISE).

The magneto-hydrodynamic simulation indicates that a super-Eddington system, which could be realized in DOGs, would produce relativistic jets (Takeuchi et al. 2010; Sadowski & Narayan 2015) and also could launch radiatively driven outflow which would eventually produce the shock-driven radio emission (e.g., Zakamska & Greene 2014). Since previous high Eddington AGN sources were searched mostly by optical (e.g., Kelly & Shen 2013), an efficient method to search for radio-loud, super-Eddington AGN/DOGs potentially opens up new access to the putative population.

In this letter, we report a finding of one radio-loud DOG J1406+0102 at  $z = 0.236$ , which shows a super-Eddington accretion signature both from the optical spectral analysis and wide-range optical-to-IR spectral energy distribution (SED) analysis. We also report that super-Eddington radio-loud DOGs could be an ideal

environment for neutrino production by  $pp$  interaction (e.g., Murase & Waxman 2016). IceCube Collaboration has been detecting cosmic high-energy neutrinos with an energy range of 30 TeV to a few PeV, majority of which most likely originate from extragalactic sources (e.g., IceCube Collaboration 2013; Abbasi et al. 2022). Recently, IceCube Collaboration reported a radio-loud AGN and an AGN with dusty environment as cosmic neutrino source candidates (e.g., IceCube Collaboration et al. 2018, 2022). We discuss the possibility to detect neutrinos from J1406+0102 and their contribution to the cosmic neutrino background.

Throughout the paper, we adopt standard cosmological parameters ( $H_0 = 70.0 \text{ km s}^{-1} \text{ Mpc}^{-1}$ ,  $\Omega_M = 0.3$ , and  $\Omega_\Lambda = 0.7$ ), translating to a scale of 3.75 kpc per arcsec at  $z = 0.236$  of J1406+0102.

## 2. DATA AND ANALYSIS

Radio-loud DOG J1406+0102 (hereafter J1406) was identified as one of the 29 radio-loud DOGs detected in the VLA/FIRST 1.4 GHz radio survey (Helfand et al. 2015) within 1 arcsec positional matching (Fukuchi et al. in preparation), and the reader should refer to Noboriguchi et al. (2019) for the original 571 IR-bright DOGs sample. After cross-matching all radio-loud DOGs with the SDSS DR17 catalog (Abdurro'uf et al. 2022), only the brightest J1406 ( $i_{\text{AB}} = 18.45$ ) was left as the source with available optical spectra. The obtained radio flux density is 9.2 mJy at 1.4 GHz, and the radio-loudness parameter of  $\log R_{\text{obs},i} = \log(f_{1.4\text{GHz}}/f_{i \text{ band}}) = 1.8$ , which is well above the boundary of radio-loud quasar of  $\log R_{\text{obs},i} > 1$  (e.g., Ivezić et al. 2002).

Figure 1 shows multiwavelength images of J1406, including Subaru/HSC S16a optical 5 bands ( $g$ ,  $r$ ,  $i$ ,  $z$  and  $y$ ), VISTA Kilo-Degree Infrared Galaxy Survey

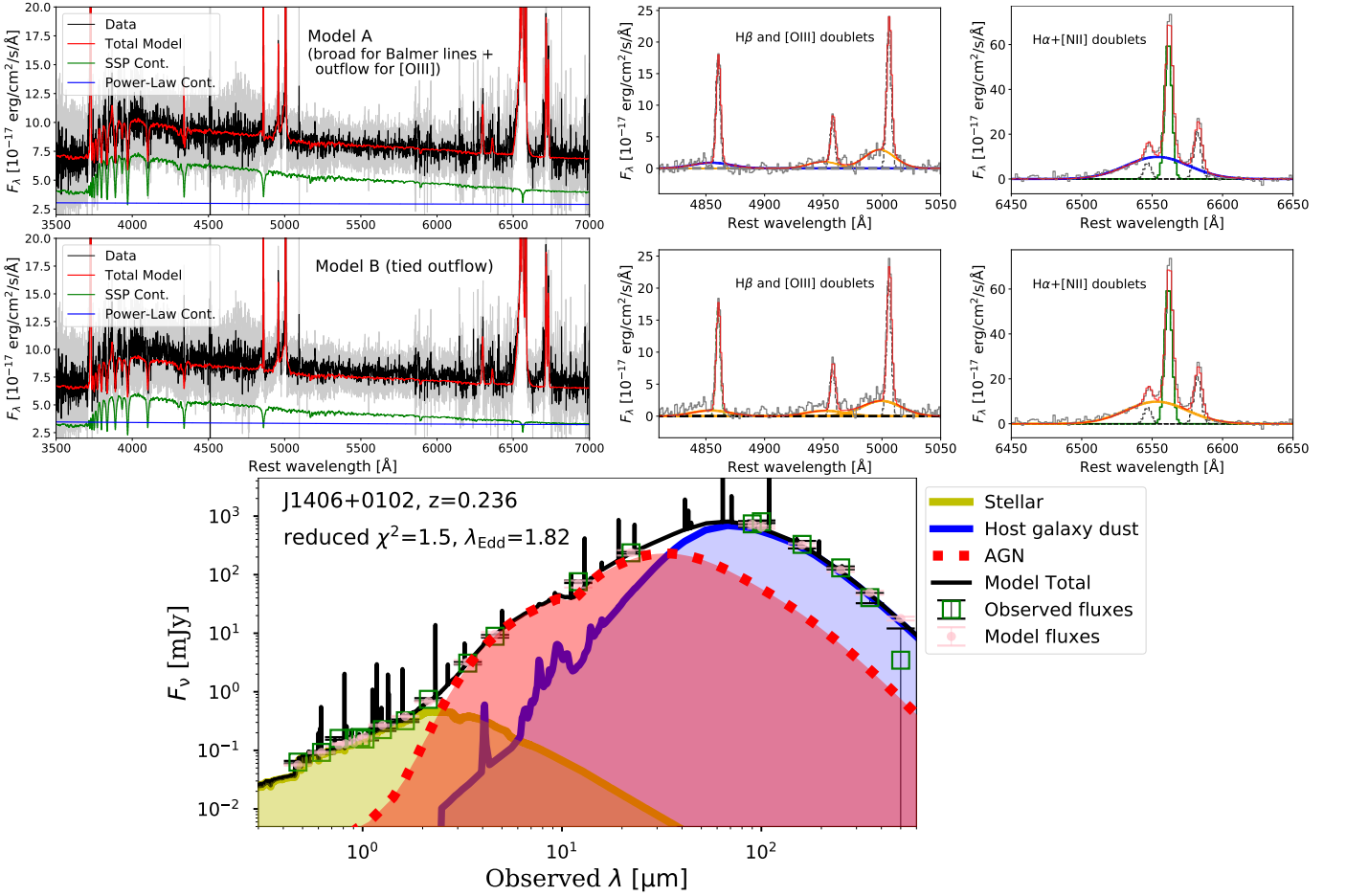


**Figure 2.** (Top) Left hand figure shows the SDSS spectrum of J1406 with fitting result using GELATO for model A: untied velocity shift and FWHM for blueshifted [O III] lines and a broad component of each Balmer line. SDSS spectrum is shown in black with 3 sigma uncertainty in grey. The simple stellar populations (SSP) continuum and power-law continuum are plotted in green and blue, respectively. The overall fit is shown in red, which include emission line models with SSP continuum and power-law continuum. (Top, middle to right) SDSS spectrum fitting results at H $\beta$ -[O III] range and H $\alpha$ -[N II] range. The spectrum is plotted as a gray line with the narrow components (gray or green dashed line), and the overall fit is shown in red. Broad H $\alpha$  and H $\beta$  Gaussian components are plotted in blue, and blueshifted [O III] component is plotted in orange. (Middle) Same figure with top panel but with a different model set-up (model B): tied velocity shift and FWHM for [O III] and Balmer lines. Right hand figure shows Broad H $\alpha$  and H $\beta$  Gaussian components and blueshifted [O III] component is plotted in orange, which have tied velocity shift and FWHM. (Bottom) SED fitting result of J1406. The red dotted line represents the AGN direct and dust emission. The blue solid line represents the dust emission from the host galaxy. The yellow line represents the stellar emission from the host galaxy and the green dashed line represents the intrinsic stellar emission. The black solid line is the combined one of dust, stellar, nebular, and AGN.

(VIKING<sup>1 2</sup>)  $Ks$  band, WISE 4 bands (W1, W2, W3 and W4; Wright et al. 2010), VLA/FIRST and VLA sky survey (VLASS, Lacy et al. 2020) images. HSC images show a clear tidal feature thanks to its high angular resolution of  $\sim 0.6$  arcsec at  $i$ -band (Aihara et al. 2018), supporting the DOGs formation scenario as a post-phase of galaxy major mergers.

<sup>1</sup> VIKING: [https://www.eso.org/sci/observing/phase3/data\\_releases/viking\\_dr2.pdf](https://www.eso.org/sci/observing/phase3/data_releases/viking_dr2.pdf)

<sup>2</sup> VIKING release note: <http://www.eso.org/rm/api/v1/public/releaseDescriptions/135>

## 2.1. SDSS Spectral Fitting

The upper left panel of Figure 2 shows the SDSS optical spectrum of J1406 (black solid line), and the middle to right panels show clear broad emission lines around the Balmer lines and [O III] $\lambda$ 4959,  $\lambda$ 5007 lines (hereafter [O III] lines). We performed the spectral fitting using GELATO code (Hviding 2022)<sup>3</sup>, which builds the composite stellar/AGN spectrum through simple stellar

<sup>3</sup> Link to the GitHub <https://github.com/TheSkytist/GELATO>

populations with an AGN power-law continuum component and AGN emission lines. The composite stellar/AGN spectrum is made following the default set of [Hviding \(2022, Table 3\)](#). Since [O III] emission lines show a strong blue-shifted component, we set full width at half-maximum (FWHM) up to  $2000 \text{ km s}^{-1}$  with the maximum velocity shift of  $1000 \text{ km s}^{-1}$  for the outflow component in the [O III] emission lines. We also set the maximum velocity shift of  $1000 \text{ km s}^{-1}$  for the broad component in Balmer lines. First, we tied FWHM and velocity shift between  $H\alpha$  and  $H\beta$  lines but not to the [O III] emission lines (Model A). The initial redshift is set as  $z = 0.2363$  obtained from the SDSS pipeline. Based on these parameter sets, we performed the SDSS spectrum fitting with 100 times bootstrap to obtain the standard deviation, and the final obtained redshift of J1406 from the stellar continuum is  $z = 0.2367$  with the reduced chi-square (reduced  $\chi^2$ ) of 1.2.

The fitting result is also shown in Figure 2 (top). The [O III] emission shows an strong blueshifted outflow feature, with the FWHM of  $770 \pm 50 \text{ km s}^{-1}$  and velocity shift of  $-550 \pm 70 \text{ km s}^{-1}$ . The broad components of the Balmer lines ( $H\beta$  and  $H\alpha$ ) show a large FWHM of  $1020 \pm 30 \text{ km s}^{-1}$  and velocity shift of  $-400 \pm 30 \text{ km s}^{-1}$ . Assuming that the Balmer broad components are virialized, we obtain the  $H\alpha$  based BH mass of  $\log(M_{\text{BH}}/M_{\odot}) = 7.30 \pm 0.25$  using equation (6) of [Greene & Ho \(2005\)](#), where the 0.25 dex error include the 0.2 dex scatter of the scaling relation and uncertainty by the spectral fitting. The extinction correction,  $E(B-V) = 1.35$ , is calculated with the Balmer decrement method applying [Calzetti et al. \(2000\)](#) extinction law and the intrinsic  $H\alpha/H\beta$  ratio of 3.06 ([Dong et al. 2008](#)) for broad components with the observed  $H\alpha$  and  $H\beta$  luminosity of  $\log(L_{H\alpha}/\text{erg s}^{-1}) = 41.99 \pm 0.01$  and  $\log(L_{H\beta}/\text{erg s}^{-1}) = 40.81 \pm 0.01$ . We note that the BH mass estimation by using the  $H\beta$  broad line is  $M_{\text{BH}} \sim 10^{7.4} M_{\odot}$ , which is consistent with the  $H\alpha$  based one. The estimated AGN bolometric luminosity ( $L_{\text{bol}}$ ) from the extinction corrected [O III] luminosity ( $L_{[\text{OIII}],\text{abs}}$ ) is  $\log(L_{\text{bol},[\text{OIII}]}/\text{erg s}^{-1}) = 45.91 \pm 0.38$ , which is consistent with the  $L_{\text{bol}}$  obtained from SED fitting (Section 2.2). Here, we assume  $L_{\text{bol},[\text{OIII}]} = 3500L_{[\text{OIII}],\text{abs}}$  with the scatter of 0.38 dex ([Heckman et al. 2004](#)), and the error of  $L_{\text{bol},[\text{OIII}]}$  is dominated by this scatter. The estimated Eddington ratio reaches  $\lambda_{\text{Edd}} = 3.3_{-2.1}^{+6.1}$ , exceeding the Eddington limit.

In contrast, there is a possibility that the broad components of Balmer lines are not virialized, and it can be related to the outflow launched from the accretion disk. We examine this possibility by adding an outflow component for each Balmer line, fixed with the same

**Table 1.** Models and the Values for Free parameters Used by CIGALE for the SED Fitting of J1406 and the Values Selected as the Best Model.

Model-Parameter	Values	Select
SFH: delayed SFH with a $\tau$ decay burst		
$\tau$ of the main population (Myr)	1000, 3000, 5000	5000
Age of the main population (Myr)	1000, 3000, 5000	1000
	10,000	
$\tau$ of the starburst population (Myr)	30, 100	100
Age of the late burst (Myr)	10, 30, 100	10
Mass fraction of burst population	0.001,0.01,0.1,0.3	0.3
Stellar population synthesis model: (1) and (2)		
Metallicity (Z)	0.4 $Z_{\odot}$ , $Z_{\odot}$	$Z_{\odot}$
Dust attenuation: (3).		
E(B-V) for young stars continuum	0.2-2.0 (step 0.3)	1.1
E(B-V) old factor	0.1, 0.3, 0.9	0.1
Dust emission: (4)		
$\alpha$ slope (IR power-law slope)	0.75	
AGN (UV-to-IR): SKIRTOR (5).		
Viewing angle ( $\theta$ )	30°, 70°	70°
AGN fraction in total IR luminosity	0.01, 0.3, 0.5, 0.7, 0.9	0.5
Extinction law of polar dust	SMC	
E(B-V) of polar dust	0.03, 0.1, 0.15	0.03
Temperature of polar dust (K)	100, 200, 300	200

References: (1) [Bruzual & Charlot \(2003\)](#); (2) [Chabrier \(2003\)](#); (3) [Calzetti et al. \(2000\)](#); (4) [Dale et al. \(2014\)](#); (5) [Stalevski et al. \(2016\)](#).

velocity shift and FWHM of the [O III] outflow component (Model B). The obtained reduced  $\chi^2$  of 1.25 is comparable to that obtained from spectral fitting with a broad Balmer component. In this case, J1406 is a type-2 AGN with strong ionized outflows (FWHM =  $1000 \pm 30 \text{ km s}^{-1}$ . and  $v_{\text{shift}} = 420 \pm 20 \text{ km s}^{-1}$ ), and BH mass estimation based on the single-epoch method may be not applicable for J1406, and a stellar mass-based BH mass estimation becomes more important (see Section 2.2).

## 2.2. Optical-FIR SED Fitting

We apply the SED decomposition method to obtain the AGN and host galaxy components by using the CIGALE SED fitting code (e.g., [Yang et al. 2022](#)), which builds the composite stellar/AGN spectrum through simple stellar populations (SSP) with flexible star-formation history (SFH) and AGN radiation.



In this study, we utilize the most up-to-date version called the CIGALE 2022.0 (hereafter CIGALE) code (Yang et al. 2022). We use the same models with Fukuchi et al. (2022), which characterized the SED of a quasar with strong starbursts and share similar conditions of AGN and host galaxy with J1406. We adopt the Chabrier (2003) initial mass function (IMF). The models and grid of parameters we used in our analysis are summarized in Table 1, and other parameters not mentioned are the same as CIGALE default values.

Under the parameter setting, we have conducted SED fitting to 18 photometric points of J1406 covering from optical to 500  $\mu\text{m}$ ; Subaru HSC 5 broadband filters, VIKING  $J$ ,  $H$ , and  $Ks$ -bands, WISE 4 bands data, AKARI FIS 90 $\mu\text{m}$  (Kawada et al. 2007), and Herschel Astrophysical Terahertz Large Area Survey (H-ATLAS; Pilbratt et al. 2010) 100, 160, 250, 350, and 500  $\mu\text{m}$ .

Figure 2 (bottom) shows the SED fitting result for the best model of J1406 by CIGALE, with the decomposed AGN (red dotted line), stellar (yellow solid line), and host dust (blue solid line) components. The SED fitting provides the total stellar mass of  $\log(M_*/M_\odot) = 9.94 \pm 0.02$ . This stellar mass corresponds to the BH mass of  $\log(M_{\text{BH}}/M_\odot) = 7.51 \pm 0.28$  by using the local scaling relation between  $M_{\text{BH}}$  and the bulge mass (Kormendy & Ho 2013) with assuming the total stellar mass as bulge mass for J1406. We also use the redshift evolutionary trend of Merloni et al. (2010), with  $M_{\text{BH}}/M_* \propto (1+z)^{0.68}$ . The estimated BH mass obtained by the scaling relation is also roughly consistent with the  $H\alpha$  based value in Section 2.1. The CIGALE fitting also gives the AGN bolometric luminosity of  $\log(L_{\text{AGN,bol}}/\text{erg s}^{-1}) = 45.87 \pm 0.02$ , resulting in Eddington ratio of  $\lambda_{\text{Edd}} = 1.82^{+1.81}_{-0.91} \gtrsim 1$ . Based on the results above, our main conclusion is that J1406 is in a super-Eddington accretion phase by using both SDSS spectral fitting and SED fitting methods. This result also supports the idea that the radio-loud DOGs search would be a good pathway to find rapidly growing SMBHs in a dust-obscured phase. This is further discussed in the following paper (Fukuchi et al. in preparation), and Noboriguchi et al. (2022) also reported some super-Eddington BHs among our DOGs sample.

### 3. DISCUSSION

#### 3.1. Origin of Radio Emission

Our results strongly indicate that J1406 has a central engine reaching the super-Eddington accretion. An interesting point is that J1406 also shows prominent radio emissions observed both in VLA/FIRST (1.4 GHz) and VLASS survey  $\sim 3$  GHz (S-band: 2–4 GHz: Lacy et al. 2020) with  $L_{1.4\text{GHz}} = 2.0 \times 10^{40}$  erg s $^{-1}$ . There are

possible origins of such radio emissions; 1) star formation, 2) radio jet, and 3) outflow-driven shock. Here, we discuss which origin(s) is a likely scenario.

##### 3.1.1. Star Formation

Host galaxies are not radio silent. They produce both synchrotron radiation from supernova remnants and free-free emission from HII regions, whose luminosities depend on the host galaxy SFR. The star formation rate for J1406 is estimated from the SED fitting with  $\log(\text{SFR}/M_\odot \text{ yr}^{-1}) = 2.31 \pm 0.02$ . The expected radio emission is  $L_{1.4\text{GHz,SF}} = (1.81 \times 10^{37} \times (\text{SFR}/M_\odot \text{ yr}^{-1})) \text{ erg s}^{-1} = 3.7 \times 10^{39} \text{ erg s}^{-1}$  (Bell 2003), which could contribute  $\sim 20\%$  of the total radio emission at 1.4 GHz, which is not enough to account for the total radio flux. This indicates that a significant fraction of the radio emission should originate either from the AGN radio jet and/or outflow-driven shock.

##### 3.1.2. Radio Jet

Theoretical simulations predict that a super-Eddington accreting BH would produce a radiation-driven radio jet (e.g., Takeuchi et al. 2010). J1406 shows a compact VLASS image within the size of the 2.5 arcsec or 4.7 kpc radius at 3 GHz (Figure 1). If J1406 has a jet, the estimated kinematic age of the jet is  $\sim 1.5 \times 10^5$  yr, by assuming the jet size of 4.7 kpc, jet angle to the line of sight of  $45^\circ$ , and a typical expansion speed of radio lobes ( $\sim 0.2c$ ; Nagai et al. 2006). This relatively young jet (compared to FRI/II sources of  $\sim 10^8$  yr) is consistent with the one launched in the current super-Eddington phase, which would last only the order of Myr (e.g., Kawaguchi et al. 2004; Eilers et al. 2020; Shirakata et al. 2020; Inayoshi et al. 2022). This young jet age also agrees with the properties of called giga-hertz peaked spectrum (GPS) radio galaxies, which have AGN jets with a linear size of 0.1–1 kpc and the radio emission is located in the environment of highly obscured gas (e.g., O’Dea 1998). Indeed, the radio spectral index of J1406 shows a relatively flat slope of  $\alpha = -0.2$  for  $S_\nu \propto \nu^\alpha$  between 1.4 GHz and 3 GHz that may be too flat compared with the extended optically thin emission (O’Dea 1998), indicating synchrotron self absorption (SSA) at  $\sim$  GHz range, which is consistent with the highly obscured gas environment of DOGs. In addition, the Tata Institute of Fundamental Research Giant Meterwave Radio Telescope Sky Survey (TGSS; Intema et al. 2017) do not detect J1406 by the  $7\sigma$  level at 150 MHz. This implies that the spectral index between 150 MHz and 1.4 GHz is harder than  $\alpha \gtrsim 0$  using the median  $3\sigma$  limit of 10.5 mJy on the TGSS flux density, further supporting the SSA-thick environment.

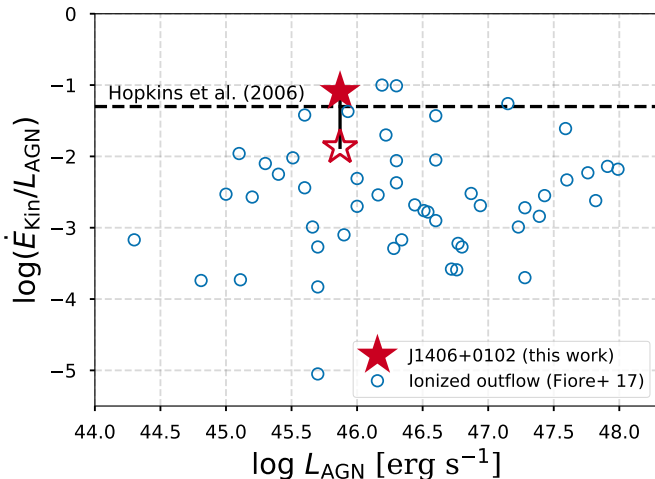


**Figure 3.** Efficiency of kinetic luminosity,  $\eta_{\text{kin}} = E_{\text{kin}}/(L_{\text{bol,AGN}}\tau)$ , as a function of bolometric AGN luminosity for J1406 together with the AGN sample with wide luminosity range compiled by Fiore et al. (2017). The lowest  $\eta_{\text{kin}}$  of J1406 is estimated using ionized gas radius of  $R = 6$  kpc. Cosmological simulation require  $\sim 5\%$  of radiation energy couples with ISM (black dashed line) to reproduce observed non-stat forming massive galaxies, and J1406 can exceed/comparable to this value.

The radio luminosity of J1406 corresponds to the jet power of  $L_{\text{jet}} \sim 10^{44}$  erg s $^{-1}$  (Cavagnolo et al. 2010), which is  $\sim 1\%$  of the radiation energy,  $L_{\text{jet}}/L_{\text{AGN,bol}} \sim 0.01$ . This jet efficiency is slightly smaller than the typical SDSS radio-loud quasars of 3-40% (e.g., Inoue et al. 2017) and the case for rapidly spinning BH of 100% (Tchekhovskoy et al. 2011), indicating J1406 may still have a small BH spin with the BH mass and spin assembly phase.

### 3.1.3. Outflow-driven Radio Shock

Some studies suggest that rapidly accreting system around SMBHs could launch radiatively driven outflows that propagate into the interstellar medium with shock, and it would eventually produce shock-driven radio emission due to synchrotron radiation (e.g., Zakamska & Greene 2014).

Utilizing the [O III] ionized gas outflow, one can estimate the contribution on such outflow-driven radio emission (e.g., Zakamska & Greene 2014). Hwang et al. (2018) showed a tight correlation between the radio luminosity and the [O III] outflow velocity of  $\log(L_{1.4\text{GHz,outflow}}/\text{erg s}^{-1}) = 2 \times \log(w_{90}/\text{km s}^{-1}) + 33.80$ , where  $w_{90}$  is the 90% enclosed velocity and  $w_{90} \sim 1.3 \times \text{FWHM}$  for the Gaussian distribution. In the case of J1406,  $w_{90} = 1080$  km s $^{-1}$  and the estimated 1.4 GHz radio luminosity reaches  $\log(L_{1.4\text{GHz,outflow}}/\text{erg s}^{-1}) = 39.87 \pm 0.56$ , which could describe the observed 1.4 GHz radio luminosity for J1406 of  $\log(L_{1.4\text{GHz}}/\text{erg s}^{-1}) =$

40.30 within a scatter. Thus, most of the radio emissions would originate from the AGN activity either from the jet and/or outflows, and in either case, bright radio emissions for DOGs can be a good indicator of rapidly growing SMBHs that reach super-Eddington accretion.

### 3.2. AGN outflow and feedback

Our results on the optical spectral fitting show that J1406 has a strong ionized [O III] outflow. This ionized gas velocity well exceeds the escaping velocity of the galaxy halo with the stellar mass of J1406 of  $\log(M_{\star}/M_{\odot}) = 9.94 \pm 0.02$  (e.g., Moster et al. 2013; Chen et al. 2020). This indicates that the super-Eddington phase of J1406 (and possibly the radio-loud DOGs in general) has a strong impact on the host galaxy growth by injecting a large amount of energy from its nucleus. Indeed, the estimated kinetic energy is  $E_{\text{kin}} = M_{\text{HII}}v_{\text{outflow}}^2/2 = 2.0 \times 10^{58}$  erg with efficient conversion of the radiation energy ( $\eta_{\text{kin}}$ ) as described below. Here,  $M_{\text{HII}}$  is the mass of the ionized hydrogen obtained from outflow components of [O III] with [O III]/H $\beta$  ratio of 1.3 and an electron density of  $n_e = 200$  cm $^{-3}$  following the estimation by Fiore et al. (2017). Using the typical outflow time scale  $\tau = R/v_{\text{outflow}}$ , we obtain a high efficiency of kinetic luminosity of  $\eta_{\text{kin}} = E_{\text{kin}}/\tau L_{\text{AGN,bol}} = 8\%$  (Figure 3), where  $R$  is the ionized gas region from the center of the BH, and we assume typical value of 1 kpc as a fiducial value (e.g., Zakamska et al. 2016). In addition to this value,  $R$  can have maximum value of 6 kpc based on maximum radius of AGN dominated region for [O III] emission line (Sun et al. 2018). In this case,  $\eta_{\text{kin}}$  can be  $\sim 1\%$  (open star in Figure 3).

Figure 3 indicates that  $\eta_{\text{kin}}=1-8\%$  for J1406 is located at the upper end of the previously reported values among AGN and quasars (e.g., Fiore et al. 2017, blue open circles), whose uncertainty is also not small, up to around 1 dex. This converting efficiency is sufficient to quench the star formation in massive galaxies and it also fulfills the requirement in the cosmological simulation to reproduce the observed BH-host galaxy scaling relation (5% of radiation energy couples with ISM: e.g., Hopkins et al. 2006, black dashed line in Figure 3). Thus, our result indicates that the existence of the super-Eddington accretion phase can strongly affect the future galaxy stellar mass assembly because of its efficient feedback.

### 3.3. Future SMBH Growth of J1406

The super-Eddington phase is considered to be a crucial path for BH growth. We discuss how this phase will shape the direction of the future BH growth for

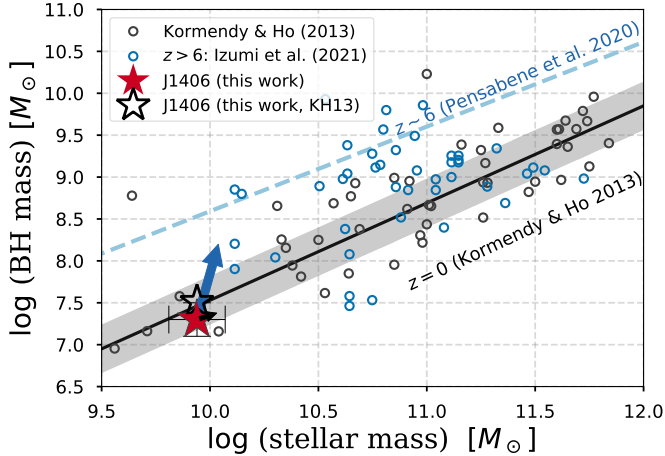


**Figure 4.** Expected future growth of J1406 in the plane of the BH mass and host stellar mass, together with the distribution of  $z > 6$  quasars compiled in Izumi et al. (2021) and those in the local universe (Kormendy & Ho 2013) with substituting dynamical/bulge mass for stellar mass. The current stellar mass and BH mass obtained from the SED fitting and spectral fitting, respectively, for J1406 is shown in red star, and black arrow shows BH growth of  $\lambda_{\text{Edd}} = 1$  with  $\eta = 0.1$  and  $\log(\text{SFR}/M_{\odot} \text{ yr}^{-1}) = 2.31$  for  $10^7$  yr. The open star represents the BH mass of J1406 using Kormendy & Ho (2013) scaling relation with correction of redshift evolution following Merloni et al. (2010). Blue arrow indicates growth of J1406 with constant Eddington ratio of  $\lambda_{\text{Edd}} = 3$  and radiation efficiency of  $\eta = 0.03$  for  $10^7$  yr. Future location in the plane will be above the local scaling relation of Kormendy & Ho (2013) (black line) by a factor of a few, which is close to the scaling relation of the high- $z$  massive quasars (blue dashed line; Pensabene et al. 2020).

J1406. The SED fitting result indicates that the BH accretion rate of  $\dot{M}_{\text{BH}} = (1 - \eta)L_{\text{AGN,bol}}/(\eta c^2) = 0.13 \times (1 - \eta)/\eta M_{\odot} \text{ yr}^{-1}$  and  $\text{SFR} = 230 M_{\odot} \text{ yr}^{-1}$ . This indicates that SMBH and host galaxy are growing with  $\dot{M}_{\text{BH}}/\text{SFR} = 1/2000 \times (1 - \eta)/\eta$ . Assuming the fiducial value of  $\eta = 0.1$  (Soltan 1982),  $\dot{M}_{\text{BH}}/\text{SFR} = 5.1 \times 10^{-3}$ . This is comparable to the local scaling relation of  $M_{\text{BH}}/M_{\star} \sim 3 \times 10^{-3}$  (Kormendy & Ho 2013).

Figure 4 shows the possible growth pathway of J1406 in the plane of  $M_{\text{BH}}$  and  $M_{\star}$  assuming the fiducial value of the standard disk of  $\eta = 0.1$ . Red circle indicates the current  $M_{\star}$  (based on the SED fitting) and  $M_{\text{BH}}$  (based on spectral analysis) of J1406, and it will grow with the direction of small black arrow when  $\lambda_{\text{Edd}} \sim 1$ ,  $\eta = 0.1$  and  $\text{SFR} = 230 M_{\odot} \text{ yr}^{-1}$  if the super-Eddington phase continue at 10 Myr (Kawaguchi et al. 2004; Shirakata et al. 2019; Inayoshi et al. 2022). This growth path roughly follows the local scaling relation as expected from the discussion above.

In contrast, super-Eddington phase has a radiatively inefficient disk (slim disk: e.g., Inayoshi et al. 2020,

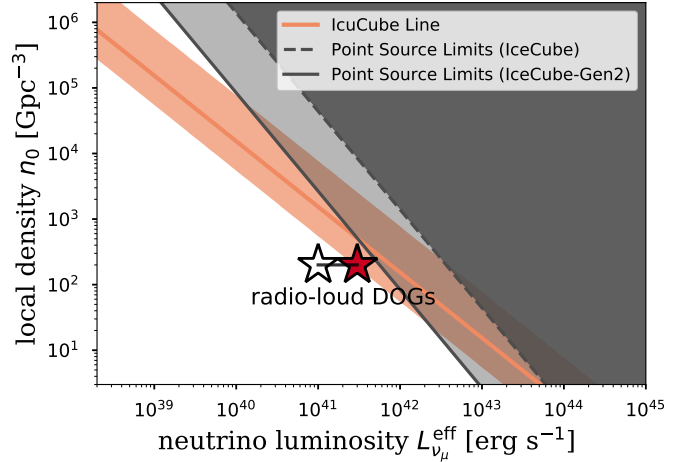


**Figure 5.** Contribution to the diffuse neutrino flux (orange shaded region) of J1406-like radio-loud DOGs (red star) and IceCube detectability (black and grey shaded region). This figure is made following Figure 3 of Murase & Waxman (2016). When the radio-loud DOGs have small reduction factor (e.g.,  $f_{\text{bol}} = 3$ ; red star, c.f.,  $f_{\text{bol}} = 10$ ; open star), they can locate in above the required  $L_{\nu_{\mu}}^{\text{eff}}$  and  $n_0$  for redshift evolution of  $\alpha = 3$  (solid line of IceCube line).

for a review), resulting in efficient growth of BH with  $\eta \leq 0.1$ . The radiation efficiency decreases into  $\eta \simeq 0.03$  (Abramowicz et al. 1988; Sadowski & Narayan 2015) at the estimated Eddington ratio for J1406 of  $\lambda_{\text{Edd}} \simeq 3$  (but see Watarai et al. 2000 for  $\eta = 0.1$  even at  $\lambda_{\text{Edd}} \simeq 3$ ). The purple arrow in Figure 4 shows the estimated future BH mass assembly of J1406, reaching  $\sim 10^8 M_{\odot}$  within  $\sim 10$  Myr. The resulting future location in the plane will move to the place above the local scaling relation of Kormendy & Ho (2013) by a factor of a few and will be closer to the scaling relation of the high- $z$  massive quasars (blue dashed line; Pensabene et al. 2020). Large Eddington ratios are more easily to occur at higher redshifts, since galaxies are more gas-rich at higher- $z$  (Shirakata et al. 2019). Thus, J1406 and other radio-loud DOGs would be a key low- $z$  ( $z < 2$ ) analogous population of rapidly growing (over-massive) high- $z$  quasar as discussed in Inayoshi et al. (2022) for super-Eddington accretion.

### 3.4. Contribution to the Cosmic Neutrino Background

J1406 and other radio-loud DOGs can have relativistic jets that can produce cosmic-rays (CRs; e.g., Kimura et al. 2018), which propagate from jet and can efficiently couple with dense ISM of DOGs, eventually producing neutrinos by  $pp$  interaction. Here, we discuss the possibility to detect neutrinos from J1406 and the contribution of radio-loud DOGs to the cosmic neutrino background, whose origin is in debates since the discovery

by IceCube Collaboration (e.g., [IceCube Collaboration 2013](#), and see Section 1).

We first discuss the detectability for J1406 by IceCube. Using the radio luminosity of J1406 and corresponding jet power of  $L_{\text{jet}} \sim 10^{44} \text{ erg s}^{-1}$  ([Cavagnolo et al. 2010](#)), we can obtain the neutrino luminosity in the IceCube band of  $L_{\nu\mu}^{\text{eff}} = \frac{1}{6}\epsilon_{\text{CR}}f_{pp}L_{\text{jet}}/f_{\text{bol}} \sim 10^{41.5} \text{ erg s}^{-1}(\epsilon_{\text{CR}}/0.1)(f_{pp}/1)(f_{\text{bol}}/3)^{-1}$ . Here, we assume the CR production rate of  $\epsilon_{\text{CR}} \sim 0.1$ , the efficiency of neutrino production of  $f_{pp} = 1$  ([Senno et al. 2015](#)) by considering the gas-rich DOGs environment and  $f_{\text{bol}} (\gtrsim 1)$  is the reduction factor to consider only the luminosity in the IceCube band. The reduction factor  $f_{\text{bol}}$  becomes close to a few, if CR has a hard spectrum (e.g., stochastic acceleration by turbulence: [Kimura et al. 2015](#)) with a large amount of flux is converted to the IceCube sensitivity range. This neutrino luminosity  $L_{\nu\mu}^{\text{eff}} \sim 10^{41.5} \text{ erg s}^{-1}$  corresponds to the neutrino flux of  $E_{\nu}^2\phi_{\nu\mu} \sim 10^{-3} \text{ GeV cm}^{-2}$  for 10 years time-integration, which is still difficult to detect even with IceCube-Gen2 ([Abbasi et al. 2022](#)).

In contrast, considering the survey area of radio-loud DOGs study of  $\sim 105 \text{ deg}^2$  ([Noboriguchi et al. 2019](#)) and one source detection at  $z = 0.2$  (this work) with the comoving volume within the reshift of  $\sim 2 \text{ Gpc}^3$ , we would have  $n_0 \sim 200 [\text{Gpc}^{-3}]$  J1406-like radio-loud DOGs in the entire sky. Figure 5 shows the required neutrino luminosity  $L_{\nu\mu}^{\text{eff}}$  and local number density  $n_0$  to account for the full diffuse neutrino flux observed by IceCube (orange shaded region), which is made following [Murase & Waxman \(2016\)](#). When the radio-loud DOGs have small reduction factor (e.g.,  $f_{\text{bol}} = 3$ ; red star, c.f.,  $f_{\text{bol}} = 10$ ; open star), they can locate in close to the required  $L_{\nu\mu}^{\text{eff}}$  and  $n_0$  for population with redshift evolution of  $n \propto (1+z)^{\alpha}$  with  $\alpha = 3$  (AGN evolution; solid line of IceCube line: [Boyle & Terlevich 1998](#)). The contribution by radio-loud DOGs can be stronger because the redshift evolution of this population might be stronger than the canonical value of  $\alpha = 3$  (e.g., evolution of flat-spectrum radio quasars; bottom line of orange shaded region in Figure 5). Using the neutrino luminosity of J1406,  $L_{\nu\mu}^{\text{eff}}$ , and local number density,  $n_0$ , we obtain the diffuse neutrino flux  $E_{\nu}^2\Phi_{\nu\mu} = \frac{c}{4\pi H_0}L_{\nu\mu}^{\text{eff}}n_0f_z = 0.4 \times 10^{-8} \text{ GeV cm}^{-2} \text{ s}^{-1} \text{ sr}^{-1} (f_z/3)(f_{\text{bol}}/3)^{-1}$ , which is comparable to the observed IceCube data of  $1.44 \times 10^{-8} (E_{\nu}/100 \text{ TeV})^{-2.37} \text{ GeV cm}^{-2} \text{ s}^{-1} \text{ sr}^{-1}$  for  $\gtrsim 100 \text{ TeV}$  ([Abbasi et al. 2022](#)). Here,  $f_z$  is the redshift evolution factor, and  $f_z = 3$  for number density evolution of  $\alpha = 3$  ([Murase & Waxman 2016](#); [Kimura 2022](#)). Thus, if most cosmic rays are converted into neutrinos at the TeV to PeV range ( $f_{\text{bol}} \sim \text{a few}$ ), J1406-like radio-loud DOGs can provide a significant contribution

to the cosmic neutrino background at the  $> 100 \text{ TeV}$  range.

This work is supported by Japan Society for the Promotion of Science (JSPS) KAKENHI (20H01939; K. Ichikawa) and KAKENHI (22K14028, 21H04487; S.S. Kimura). S.S.K. acknowledges support by the Tohoku Initiative for Fostering Global Researchers for Interdisciplinary Sciences (TI-FRIS) of MEXT's Strategic Professional Development Program for Young Researchers. We also acknowledge support from the National Natural Science Foundation of China (12073003, 12150410307, 12003003, 11721303, 11991052, 11950410493), and the China Manned Space Project Nos. CMS-CSST-2021-A04 and CMS-CSST-2021-A06.

This publication makes use of data products from the Wide-field Infrared Survey Explorer, which is a joint project of the University of California, Los Angeles, and the Jet Propulsion Laboratory/California Institute of Technology, funded by the National Aeronautics and Space Administration.



## REFERENCES

- Abbasi, R., Ackermann, M., Adams, J., et al. 2022, *ApJ*, 928, 50, doi: [10.3847/1538-4357/ac4d29](https://doi.org/10.3847/1538-4357/ac4d29)
- Abdurro'uf, Accetta, K., Aerts, C., et al. 2022, *ApJS*, 259, 35, doi: [10.3847/1538-4365/ac4414](https://doi.org/10.3847/1538-4365/ac4414)
- Abramowicz, M. A., Czerny, B., Lasota, J. P., & Szuszkiewicz, E. 1988, *ApJ*, 332, 646, doi: [10.1086/166683](https://doi.org/10.1086/166683)
- Aihara, H., Arimoto, N., Armstrong, R., et al. 2018, *PASJ*, 70, S4, doi: [10.1093/pasj/psx066](https://doi.org/10.1093/pasj/psx066)
- Bell, E. F. 2003, *ApJ*, 586, 794, doi: [10.1086/367829](https://doi.org/10.1086/367829)
- Boyle, B. J., & Terlevich, R. J. 1998, *MNRAS*, 293, L49, doi: [10.1046/j.1365-8711.1998.01264.x](https://doi.org/10.1046/j.1365-8711.1998.01264.x)
- Bruzual, G., & Charlot, S. 2003, *MNRAS*, 344, 1000, doi: [10.1046/j.1365-8711.2003.06897.x](https://doi.org/10.1046/j.1365-8711.2003.06897.x)
- Calzetti, D., Armus, L., Bohlin, R. C., et al. 2000, *ApJ*, 533, 682, doi: [10.1086/308692](https://doi.org/10.1086/308692)
- Cavagnolo, K. W., McNamara, B. R., Nulsen, P. E. J., et al. 2010, *ApJ*, 720, 1066, doi: [10.1088/0004-637X/720/2/1066](https://doi.org/10.1088/0004-637X/720/2/1066)
- Chabrier, G. 2003, *PASP*, 115, 763, doi: [10.1086/376392](https://doi.org/10.1086/376392)
- Chen, X., Akiyama, M., Ichikawa, K., et al. 2020, *ApJ*, 900, 51, doi: [10.3847/1538-4357/aba599](https://doi.org/10.3847/1538-4357/aba599)
- Dale, D. A., Helou, G., Magdis, G. E., et al. 2014, *ApJ*, 784, 83, doi: [10.1088/0004-637X/784/1/83](https://doi.org/10.1088/0004-637X/784/1/83)
- Dey, A., Soifer, B. T., Desai, V., et al. 2008, *ApJ*, 677, 943, doi: [10.1086/529516](https://doi.org/10.1086/529516)
- Dong, X., Wang, T., Wang, J., et al. 2008, *MNRAS*, 383, 581, doi: [10.1111/j.1365-2966.2007.12560.x](https://doi.org/10.1111/j.1365-2966.2007.12560.x)
- Eilers, A.-C., Hennawi, J. F., Decarli, R., et al. 2020, *ApJ*, 900, 37, doi: [10.3847/1538-4357/aba52e](https://doi.org/10.3847/1538-4357/aba52e)
- Fiore, F., Feruglio, C., Shankar, F., et al. 2017, *A&A*, 601, A143, doi: [10.1051/0004-6361/201629478](https://doi.org/10.1051/0004-6361/201629478)
- Fukuchi, H., Ichikawa, K., Akiyama, M., et al. 2022, arXiv e-prints, arXiv:2209.09255, <https://arxiv.org/abs/2209.09255>
- Greene, J. E., & Ho, L. C. 2005, *ApJ*, 630, 122, doi: [10.1086/431897](https://doi.org/10.1086/431897)
- Greene, J. E., Strader, J., & Ho, L. C. 2020, *ARA&A*, 58, 257, doi: [10.1146/annurev-astro-032620-021835](https://doi.org/10.1146/annurev-astro-032620-021835)
- Heckman, T. M., Kauffmann, G., Brinchmann, J., et al. 2004, *ApJ*, 613, 109, doi: [10.1086/422872](https://doi.org/10.1086/422872)
- Helfand, D. J., White, R. L., & Becker, R. H. 2015, *ApJ*, 801, 26, doi: [10.1088/0004-637X/801/1/26](https://doi.org/10.1088/0004-637X/801/1/26)
- Hopkins, P. F., Hernquist, L., Cox, T. J., et al. 2006, *ApJS*, 163, 1, doi: [10.1086/499298](https://doi.org/10.1086/499298)
- Hopkins, P. F., Hernquist, L., Cox, T. J., & Kereš, D. 2008, *ApJS*, 175, 356, doi: [10.1086/524362](https://doi.org/10.1086/524362)
- Hviding, R. E. 2022, TheSkyentist/GELATO: GELATO v.2.5.1, v2.5.1, Zenodo, Zenodo, doi: [10.5281/zenodo.5999213](https://doi.org/10.5281/zenodo.5999213)
- Hwang, H.-C., Zakamska, N. L., Alexandroff, R. M., et al. 2018, *MNRAS*, 477, 830, doi: [10.1093/mnras/sty742](https://doi.org/10.1093/mnras/sty742)
- IceCube Collaboration. 2013, *Science*, 342, 1242856, doi: [10.1126/science.1242856](https://doi.org/10.1126/science.1242856)
- IceCube Collaboration, Aartsen, M. G., Ackermann, M., et al. 2018, *Science*, 361, eaat1378, doi: [10.1126/science.aat1378](https://doi.org/10.1126/science.aat1378)
- IceCube Collaboration, Abbasi, R., Ackermann, M., et al. 2022, *Science*, 378, 538, doi: [10.1126/science.abg3395](https://doi.org/10.1126/science.abg3395)
- Inayoshi, K., Nakatani, R., Toyouchi, D., et al. 2022, *ApJ*, 927, 237, doi: [10.3847/1538-4357/ac4751](https://doi.org/10.3847/1538-4357/ac4751)
- Inayoshi, K., Visbal, E., & Haiman, Z. 2020, *ARA&A*, 58, 27, doi: [10.1146/annurev-astro-120419-014455](https://doi.org/10.1146/annurev-astro-120419-014455)
- Inoue, Y., Doi, A., Tanaka, Y. T., Sikora, M., & Madejski, G. M. 2017, *ApJ*, 840, 46, doi: [10.3847/1538-4357/aa6b57](https://doi.org/10.3847/1538-4357/aa6b57)
- Intema, H. T., Jagannathan, P., Mooley, K. P., & Frail, D. A. 2017, *A&A*, 598, A78, doi: [10.1051/0004-6361/201628536](https://doi.org/10.1051/0004-6361/201628536)
- Ivezić, Ž., Menou, K., Knapp, G. R., et al. 2002, *AJ*, 124, 2364, doi: [10.1086/344069](https://doi.org/10.1086/344069)
- Izumi, T., Matsuoka, Y., Fujimoto, S., et al. 2021, *ApJ*, 914, 36, doi: [10.3847/1538-4357/abf6dc](https://doi.org/10.3847/1538-4357/abf6dc)
- Kawada, M., Baba, H., Barthel, P. D., et al. 2007, *PASJ*, 59, S389, doi: [10.1093/pasj/59.sp2.S389](https://doi.org/10.1093/pasj/59.sp2.S389)
- Kawaguchi, T., Aoki, K., Ohta, K., & Collin, S. 2004, *A&A*, 420, L23, doi: [10.1051/0004-6361:20040157](https://doi.org/10.1051/0004-6361:20040157)
- Kelly, B. C., & Shen, Y. 2013, *ApJ*, 764, 45, doi: [10.1088/0004-637X/764/1/45](https://doi.org/10.1088/0004-637X/764/1/45)
- Kimura, S. S. 2022, arXiv e-prints, arXiv:2202.06480, doi: [10.48550/arXiv.2202.06480](https://doi.org/10.48550/arXiv.2202.06480)
- Kimura, S. S., Murase, K., & Toma, K. 2015, *ApJ*, 806, 159, doi: [10.1088/0004-637X/806/2/159](https://doi.org/10.1088/0004-637X/806/2/159)
- Kimura, S. S., Murase, K., & Zhang, B. T. 2018, *PhRvD*, 97, 023026, doi: [10.1103/PhysRevD.97.023026](https://doi.org/10.1103/PhysRevD.97.023026)
- Kormendy, J., & Ho, L. C. 2013, *ARA&A*, 51, 511, doi: [10.1146/annurev-astro-082708-101811](https://doi.org/10.1146/annurev-astro-082708-101811)
- Lacy, M., Baum, S. A., Chandler, C. J., et al. 2020, *PASP*, 132, 035001, doi: [10.1088/1538-3873/ab63eb](https://doi.org/10.1088/1538-3873/ab63eb)
- Merloni, A., Bongiorno, A., Bolzonella, M., et al. 2010, *ApJ*, 708, 137, doi: [10.1088/0004-637X/708/1/137](https://doi.org/10.1088/0004-637X/708/1/137)
- Miyazaki, S., Komiyama, Y., Kawanomoto, S., et al. 2018, *PASJ*, 70, S1, doi: [10.1093/pasj/psx063](https://doi.org/10.1093/pasj/psx063)
- Moster, B. P., Naab, T., & White, S. D. M. 2013, *MNRAS*, 428, 3121, doi: [10.1093/mnras/sts261](https://doi.org/10.1093/mnras/sts261)
- Murase, K., & Waxman, E. 2016, *PhRvD*, 94, 103006, doi: [10.1103/PhysRevD.94.103006](https://doi.org/10.1103/PhysRevD.94.103006)
- Nagai, H., Inoue, M., Asada, K., Kameno, S., & Doi, A. 2006, *ApJ*, 648, 148, doi: [10.1086/505793](https://doi.org/10.1086/505793)

- Noboriguchi, A., Nagao, T., Toba, Y., et al. 2019, *ApJ*, 876, 132, doi: [10.3847/1538-4357/ab1754](https://doi.org/10.3847/1538-4357/ab1754)
- . 2022, *ApJ*, 941, 195, doi: [10.3847/1538-4357/aca403](https://doi.org/10.3847/1538-4357/aca403)
- O’Dea, C. P. 1998, *PASP*, 110, 493, doi: [10.1086/316162](https://doi.org/10.1086/316162)
- Pensabene, A., Carniani, S., Perna, M., et al. 2020, *A&A*, 637, A84, doi: [10.1051/0004-6361/201936634](https://doi.org/10.1051/0004-6361/201936634)
- Pilbratt, G. L., Riedinger, J. R., Passvogel, T., et al. 2010, *A&A*, 518, L1, doi: [10.1051/0004-6361/201014759](https://doi.org/10.1051/0004-6361/201014759)
- Sadowski, A., & Narayan, R. 2015, *MNRAS*, 453, 3213, doi: [10.1093/mnras/stv1802](https://doi.org/10.1093/mnras/stv1802)
- Senno, N., Mészáros, P., Murase, K., Baerwald, P., & Rees, M. J. 2015, *ApJ*, 806, 24, doi: [10.1088/0004-637X/806/1/24](https://doi.org/10.1088/0004-637X/806/1/24)
- Shirakata, H., Kawaguchi, T., Okamoto, T., Nagashima, M., & Oogi, T. 2020, *ApJ*, 898, 63, doi: [10.3847/1538-4357/ab9949](https://doi.org/10.3847/1538-4357/ab9949)
- Shirakata, H., Kawaguchi, T., Oogi, T., Okamoto, T., & Nagashima, M. 2019, *MNRAS*, 487, 409, doi: [10.1093/mnras/stz1282](https://doi.org/10.1093/mnras/stz1282)
- Soltan, A. 1982, *MNRAS*, 200, 115, doi: [10.1093/mnras/200.1.115](https://doi.org/10.1093/mnras/200.1.115)
- Stalevski, M., Ricci, C., Ueda, Y., et al. 2016, *MNRAS*, 458, 2288, doi: [10.1093/mnras/stw444](https://doi.org/10.1093/mnras/stw444)
- Sun, A.-L., Greene, J. E., Zakamska, N. L., et al. 2018, *MNRAS*, 480, 2302, doi: [10.1093/mnras/sty1394](https://doi.org/10.1093/mnras/sty1394)
- Takeuchi, S., Ohsuga, K., & Mineshige, S. 2010, *PASJ*, 62, L43, doi: [10.1093/pasj/62.5.L43](https://doi.org/10.1093/pasj/62.5.L43)
- Tchekhovskoy, A., Narayan, R., & McKinney, J. C. 2011, *MNRAS*, 418, L79, doi: [10.1111/j.1745-3933.2011.01147.x](https://doi.org/10.1111/j.1745-3933.2011.01147.x)
- Toba, Y., Nagao, T., Strauss, M. A., et al. 2015, *PASJ*, 67, 86, doi: [10.1093/pasj/psv057](https://doi.org/10.1093/pasj/psv057)
- Toba, Y., Nagao, T., Kajisawa, M., et al. 2017, *ApJ*, 835, 36, doi: [10.3847/1538-4357/835/1/36](https://doi.org/10.3847/1538-4357/835/1/36)
- Wang, F., Yang, J., Fan, X., et al. 2021, *ApJL*, 907, L1, doi: [10.3847/2041-8213/abd8c6](https://doi.org/10.3847/2041-8213/abd8c6)
- Watarai, K.-y., Fukue, J., Takeuchi, M., & Mineshige, S. 2000, *PASJ*, 52, 133, doi: [10.1093/pasj/52.1.133](https://doi.org/10.1093/pasj/52.1.133)
- Wright, E. L., Eisenhardt, P. R. M., Mainzer, A. K., et al. 2010, *AJ*, 140, 1868, doi: [10.1088/0004-6256/140/6/1868](https://doi.org/10.1088/0004-6256/140/6/1868)
- Yang, G., Boquien, M., Brandt, W. N., et al. 2022, *ApJ*, 927, 192, doi: [10.3847/1538-4357/ac4971](https://doi.org/10.3847/1538-4357/ac4971)
- Zakamska, N. L., & Greene, J. E. 2014, *MNRAS*, 442, 784, doi: [10.1093/mnras/stu842](https://doi.org/10.1093/mnras/stu842)
- Zakamska, N. L., Hamann, F., Pâris, I., et al. 2016, *MNRAS*, 459, 3144, doi: [10.1093/mnras/stw718](https://doi.org/10.1093/mnras/stw718)